DESIGN OF THE RF PHASE AND AMPLITUDE CONTROL SYSTEM FOR A PROTON LINEAR ACCELERATOR*

Robert A. Jameson, Thomas F. Turner, Ned A. Lindsay

University of California, Los Alamos Scientific Laboratory
Los Alamos, New Mexico

Summary

The specifications on RF amplitude and phase in a proton linear accelerator are reviewed. The expected amplitude and phase disturbances during normal operation are discussed, showing the need for fast control of these parameters during the beam-on period. Analytical expressions are derived for the response of the RF amplitude and phase envelopes in an accelerator structure to amplitude or phase modulations in the drive. Experimental results verifying the theoretical expressions are presented.

Introduction

In a proton linear accelerator, the phase and amplitude of the RF field supplied to the accelerating structure by the RF system determine the proton motion in the accelerator. Thus specification of the fluctuations which these parameters can be allowed to make from the design values must come directly from studies of accelerator beam dynamics.

Specification studies are being made[1] by correlating the statistical uncertainty of particle bunch location in phase space with random errors in the cell-to-cell and tank-to-tank RF amplitudes and phases. Present results indicate that whenever beam is in the machine, the average tank-to-tank amplitudes and phases must be held to within about ±1% and ±2° respectively of the design values.

An investigation has been made of the types of amplitude and phase disturbances which will affect the machine under normal operation. The major effects will be systematic perturbations caused by the proton beam as it is turned on and loads the cavity. To compensate for this loading, the input power to the cavity must be increased up to 40%, and phase must be adjusted to account for the synchronous phase of the beam with respect to the RF. A phase correction must also be made to compensate for reduced transit time in the high power amplifier due to an increase in output. Thus, phase and amplitude disturbances on the order of 15° and 20% respectively are expected to occur during each pulse, indicating the need for fast control systems operating continuously during each pulse.

It is expected that phase changes will also occur due to temperature effects, but these could be corrected by a slow phase control system. Short term phase and amplitude jitter due to random noise phenomena in the reference source, RF amplifiers, and associated equipment should not be a problem if the signal-to-noise ratio is at least 40 db at all points in the system.

* Work sponsored by the U.S. Atomic Energy Commission

The proposed control systems are shown in block diagram form in Fig. 1. Notice that the RF power amplifiers and the accelerator tanks are common to both loops and cause interaction between them.

The remainder of this paper is devoted to an analysis of RF field transient behavior in an 805-Mc accelerator structure. This information is essential before a control system can be designed since the field is the controlled variable. Experimental results obtained using a phase detector and phase shifter proposed for the control system are presented in verification of the theory.

The other elements in the control loops have also been studied. Preliminary designs have been completed, using linear theory since the expected disturbances are small. Several designs have been found which are stable and ready for experimental trials.

Transient Behavior of Loaded-Waveguide Standing-Wave Structures

The equivalent circuit approach to the analysis of coupled cell behavior has been used extensively at Los Alamos[2] to investigate steady state phenomena. It is also useful as a guide to transient behavior. A singly-resonant lumped parameter equivalent circuit for the accelerator cavity is shown in Fig. 2. This circuit is adequate to explain the behavior of more complicated doubly resonant structures also, if effective parameters are chosen to match the dispersion curves in the region about the operating point.

The tank transfer functions are derived from the transient analysis of this circuit, in which the cell currents are direct analogies of the cavity cell fields. The matrix equations for the circuit are written using Laplace transforms, transforming first with respect to time, and then, after using jump functions to express the repetitive nature of the cells, with respect to the cell number. The solution of the homogeneous equation gives the characteristic equation and the n-dependence. The inhomogeneous equation is then solved using the orthogonality relation based on the n-dependence. The complete solution for the current in any cell is:

$$I(s,n) = \sum_{d=0}^{N} \sum_{q=0}^{N} \left\{ \frac{2 \cos \frac{\pi nq}{N}}{N\left(1+k \cos \frac{\pi q}{N}\right)} \frac{\cos \frac{\pi dq}{N} W_1(q)\, s\, E(s,d)}{\left[s^2 + \frac{\omega_o}{Q(1+k \cos \frac{\pi q}{N})} s + \frac{\omega_o^2}{(1+k \cos \frac{\pi q}{N})} \right]} \right\} \quad (1)$$

where d = index on RF drive; e.g. E (s,d) is a drive in the d^{th} cell.
q = mode number
n = cell number
E(s,d) = drive term normalized by 1/2L
$W_1(q)$ = $\begin{cases} 1/2; & q = 0,\ q = N \\ 1; & 0 < q < N \end{cases}$

The transfer function with respect to a particular drive is:

$$\frac{I(s,n)}{E(s,d)} = \sum_{q=0}^{N} \left\{ \frac{2 \cos \frac{\pi nq}{N} \cos \frac{\pi dq}{N} W_1(q)}{N\left(1 + k \cos \frac{\pi q}{N}\right)} \cdot \frac{s}{\left[s^2 + \frac{\omega_o}{Q\left(1+k \cos \frac{\pi q}{N}\right)} s + \frac{\omega_o^2}{\left(1+k \cos \frac{\pi q}{N}\right)} \right]} \right\} \quad (2)$$

Example

The time response of a high Q structure to a single sinusoidal drive in the d^{th} cell, started at t = 0, is:

$$i(t,n) \cong \sum_{q=0}^{N} K_q \left[\sin(\omega t + \Phi_\omega) + e^{-\alpha_q t} \sin(\omega_q t + \Phi_{\omega q}) \right] \quad (3)$$

where $K_q = \dfrac{2\omega W_1(q) \cos \frac{\pi dq}{N} \cos \frac{\pi nq}{N}}{N\left(\left[\omega^2 \left(1+k \cos \frac{\pi q}{N}\right) - \omega_o^2 \right]^2 + \left[\frac{\omega_o \omega}{Q} \right]^2 \right)^{1/2}}$

$$\Phi_\omega = \tan^{-1} \frac{-Q\left[\omega^2 \left(1+k \cos \frac{\pi q}{N}\right) - \omega_o^2 \right]}{\omega_o \omega}$$

$$\Phi_{\omega q} = \tan^{-1} \frac{2Q \sqrt{\left(1+k \cos \frac{\pi q}{N}\right)} \left[\omega^2 \left(1+k \cos \frac{\pi q}{N}\right) - \omega_o^2 \right]}{-\left[\omega^2 \left(1+k \cos \frac{\pi q}{N}\right) + \omega_o^2 \right]}$$

$$\alpha_q = \frac{\omega_o}{2Q\left(1+k \cos \frac{\pi q}{N}\right)}$$

$$\omega_q = \frac{\omega_o}{\sqrt{\left(1+k \cos \frac{\pi q}{N}\right)}}$$

The steady-state current at any particular drive frequency is the sum of components from each mode. If the drive is at a mode resonant frequency, that component has its maximum amplitude and is in phase with the drive. The other components are present because of losses in the system. They are driven far from resonance and thus have small amplitudes and are about 90° out of phase with the drive.

The transient terms show the natural frequencies and the damping factors of the system. Both amplitude and phase transients die out with the same time constants.

Envelope Responses

The responses of real interest are those of the tank phase and amplitude envelopes when phase or amplitude modulations are imposed on a sinusoidal drive. We choose to find the transfer functions which characterize these responses by working in the time domain using the above example. The solution, which gives the response to a step amplitude change in a sinusoidal drive, is rewritten in the form:

$$i(t,n) = \sum_{q=0}^{N} \mathrm{Im} \left\{ \left[a_q(t)\, e^{i\phi_q(t)} \right] e^{i\omega t} \right\} \quad (4)$$

where $a_q(t)$ = amplitude envelope function
$\phi_q(t)$ = phase envelope function

$$= \sum_{q=0}^{N} \mathrm{Im} \left\{ K_q e^{i\omega t} \left[e^{i\Phi_\omega} + e^{-\alpha_q t} e^{-i\left[(\omega-\omega_q)t - \Phi_{\omega q}\right]} \right] \right\}$$

To obtain simplified expressions for design work, the response is approximated by two components, a driven mode component and a quadrature component. The latter is found by first assuming that each off-resonance component is exactly ±90° out of phase with the driven mode component at steady state. The amplitude is then taken to be the vector sum of these steady-state terms and called ΣKq. The damping term is taken to be that of the driven mode α_N for pi-mode drive. The beat frequency $\beta = \omega - \omega_q$ is taken to be that produced by the nearest mode frequency to the drive frequency that is present in the tank.

The resulting envelope responses to pulse turn-on are:

$$a(t) = \left\{ \left[K_N(1-e^{-\alpha_N t}) + \Sigma K_q e^{-\alpha_N t} \sin \beta t \right]^2 + \left[\Sigma K_q (1-e^{-\alpha_N t} \cos \beta t) \right]^2 \right\}^{1/2} \quad (5)$$

$$\phi(t) = \tan^{-1} \frac{-\Sigma K_q (1-e^{-\alpha_N t} \cos \beta t)}{K_N(1-e^{-\alpha_N t}) + \Sigma K_q e^{-\alpha_N t} \sin \beta t} \quad (6)$$

For small modulations, both a(t) and φ(t) will be approximately linear and may be characterized by transfer functions suitable for linear control system design studies. To find these, we impose in turn a small amplitude step and a small phase step, represented by equivalent amplitude modulation, upon a steady-state field in the cavity. The resulting envelope responses are Laplace transformed and the transform of the modulating signal is divided out, leaving the desired transfer functions. The results are listed below for pi-mode drive.

1. Response to small amplitude step = k from steady-state; k >>1:

$$a(t) = \sqrt{K_N^2 + (\Sigma K_q)^2} \left[1 + k \left(\frac{K_N^2(1-e^{-\alpha_N t}) + K_N \Sigma K_q e^{-\alpha_N t} \sin \beta t + (\Sigma K_q)^2 (1-e^{-\alpha_N t} \cos \beta t)}{K_N^2 + (\Sigma K_q)^2} \right) \right. \quad (7)$$

$$\phi(t) = -\frac{\Sigma Kq}{K_N}\left[1 + ke^{-\alpha_N t}(1-\cos\beta t)\right]\ ;\ \frac{\Sigma Kq}{K_N} \ll 1 \qquad (8)$$

Small signal transfer functions:

$$\frac{\Delta A(s)}{\Delta E(s)} = \frac{\alpha_N\sqrt{K_N^2 + (\Sigma Kq)^2}}{s+\alpha_N} + \frac{\Sigma Kq\ \beta\ s}{(s+\alpha_N)^2+\beta^2} \qquad (9)$$

$$\frac{\Delta\phi(s)}{\Delta E(s)} = -\frac{\Sigma Kq}{K_N}\left[\frac{\beta^2 s}{(s+\alpha_N)[(s+\alpha_N)^2+\beta^2]}\right] \qquad (10)$$

2. Response to step phase change of φ radians from steady state:

$$a(t) = \Big\{K_N^2\left[1-2e^{-\alpha_N t}(1-\cos\varphi)\ (1-e^{-\alpha_N t})\right] - 2K_N\Sigma Kq\left[(1-\cos\varphi)e^{-\alpha_N t}\ (2e^{-\alpha_N t}-1)\sin\beta t - \sin\varphi e^{-\alpha_N t}(1-\cos\beta t)\right] + (\Sigma Kq)^2\left[1 - 2e^{-\alpha_N t}(\sin\varphi\sin\beta t + (1-\cos\varphi)\cos\beta t) + 2(1-\cos\varphi)\ e^{-2\alpha_N t}\right]\Big\}^{1/2} \qquad (11)$$

$$\phi(t) = \tan^{-1}\frac{K_N\left[(1-e^{-\alpha_N t})\sin\varphi\right] - \Sigma Kq\left[\cos\varphi + e^{-\alpha_N t}(1-\cos\varphi)\right] + \Sigma Kq\left[\sin\varphi + e^{-\alpha_N t}(1-\cos\varphi)\cos\beta t - \sin\varphi\sin\beta t\right]}{K_N\left[\cos\varphi + e^{-\alpha_N t}(1-\cos\varphi)\right] + \Sigma Kq\left[\sin\varphi - e^{-\alpha_N t}\left((1-\cos\varphi)\sin\beta t + \sin\varphi\cos\beta t\right)\right]} \qquad (12)$$

Small signal transfer functions:

$$\frac{\Delta A(s)}{\Delta\theta(s)} = \frac{K_N\,\Sigma Kq}{\sqrt{K_N^2 + (\Sigma Kq)^2}}\left[\frac{\beta^2 s}{(s+\alpha_N)[(s+\alpha_N)^2+\beta^2]}\right] \qquad (13)$$

$$\frac{\Delta\phi(s)}{\Delta\theta(s)} = \frac{\alpha_N}{s+\alpha_N} + \frac{\Sigma Kq}{K_N}\frac{\beta\ s}{(s+\alpha_N)^2+\beta^2} \qquad (14)$$

Exact solutions of Eq.(2) have been found using a digital computer. Figs. 4,6, and 8 show the responses of an N = 20, Q = 5000, k = 0.25 example to various drive conditions. In this example, the circuit was driven in an end cell and the responses are those of the drive cell.

The approximate responses using the two-component approximations are superimposed on the exact responses. In general, the approximate responses fit the time scale very well, but show somewhat more severe amplitude fluctuations. Thus their use introduces some safety factor in a design.

Experimental Results

The transient theory has been experimentally verified using model loaded waveguide structures.

Amplitude modulation is introduced by pulse modulating the output of a signal generator with a pin-diode absorption type modulator to minimize incidental fm effects. Amplitude response is measured directly by detecting a loop coupled output from the tank with a fast rise and fall crystal detector.

Phase modulation is introduced by pulse modulating an electronic phase shifter. Phase shift is accomplished by changing the bias voltage on a pair of varactors which form terminations on two ports of a four-port network. The unit has a switching speed of about 30 nsec, and a modulation response to sinusoidal bias modulation which is flat to at least 10 Mc.

Phase response is measured with an experimental phase detection bridge[3], shown in Fig. 3. The heart of the bridge is a square coaxial bridge one-quarter wavelength on each side. An RF reference signal E_2 and an unknown signal E_1 are the inputs to the bridge, and a mixture of these signals is detected at the other two ports. Subject to the condition $|E_1| \gg |E_2|$ and linear detection, the two outputs are differenced to form the error signal, which is proportional to $|E_2|$ but not $|E_1|$ and the sine of the phase difference between E_1 and E_2. For non-linear detection, the output depends on $|E_1|$ also.

Detector match is the most serious problem with this bridge. The present detectors are 6173 pencil diodes with heated filaments. These have been found to track very well over a 50-db input power range in a suitable mount[4] with video loads of 50-100 ohms. The detection law under these conditions is 1.3. Thus, the bridge output must be corrected for amplitude changes in the unknown signal. This will not be a problem in the intended control application, since the field amplitude will be constant within about 1%.

Figures 5,7,9, and 10 show representative responses found experimentally which correspond to the analytical responses shown in Figs. 4, 6, and 8. The qualitative agreement is excellent in every case.

Quantitatively, the agreement with Eqs. (5), (11), and (12) is within about 5%, which is the estimated limit on present measurement error. The agreement with Eq.(6) is very difficult to measure, because it alone of the four responses of interest is completely dependent on the excitation of other modes during transients. The extent of this excitation is difficult to measure on a real cavity with errors in the cells. However, a fit to the maximum deflection is adequate for control studies.

Conclusion

The analytical expressions needed to describe RF field phase and amplitude transients in coupled cells have been obtained. Experimental results show good quantitative agreement except in the case of phase response to a large amplitude change, for which a fit to measured response should be made for final design work.

References

1. H. S. Butler, "Linac Error Analysis by Matrix Methods," to be presented to APS Meeting, Washington, D. C., April, 1965.
2. E. A. Knapp, "Design, Construction and Testing of RF Structures for a Proton Linear Accelerator, B-5, this conference.
3. L. B. Mullett, "A Matrix Treatment of Four-Arm Bridges," A.E.R.E. (Harwell), Report No. GP/R 1578, 1955.
4. C. Brian Williams, "Design Report - Automatic Phasing System for High Power Klystrons," SLAC, 1963.

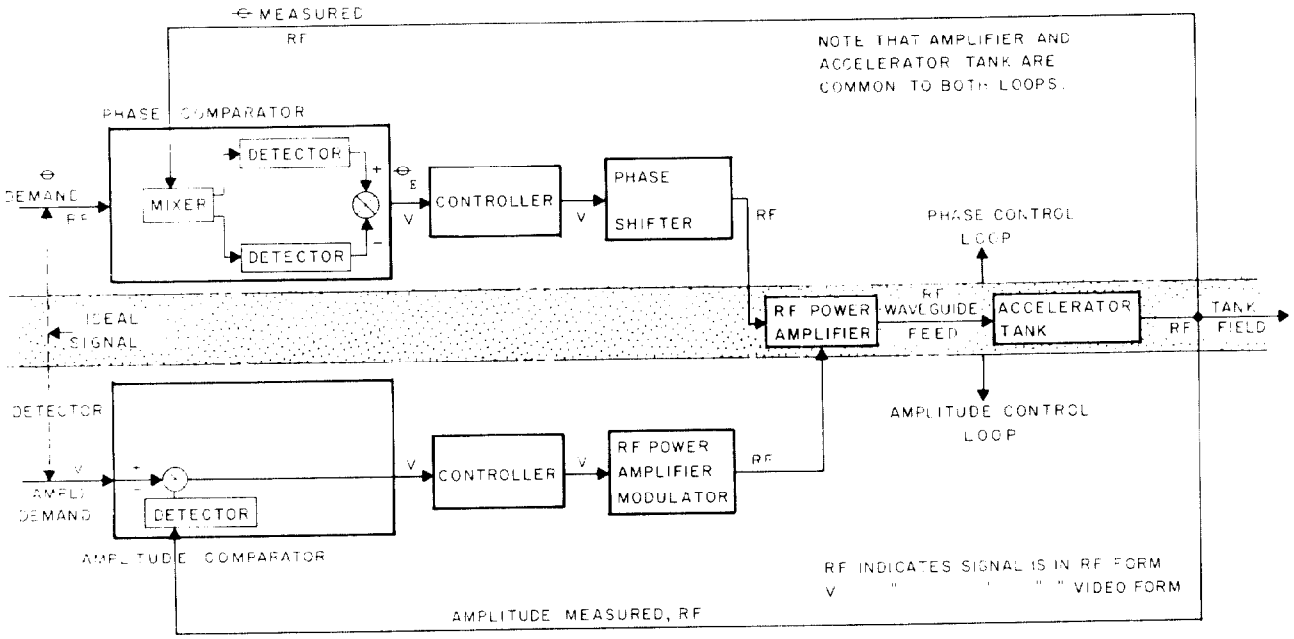

Fig. 1. Block diagram of the RF phase and amplitude control loops.

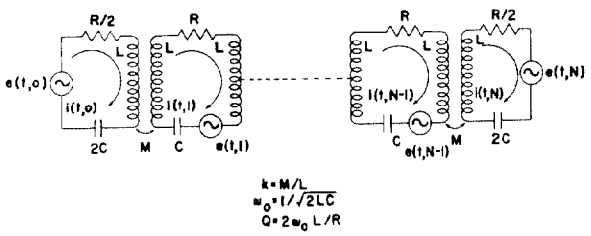

Fig. 2. Equivalent circuit for the 805-Mc accelerator structure.

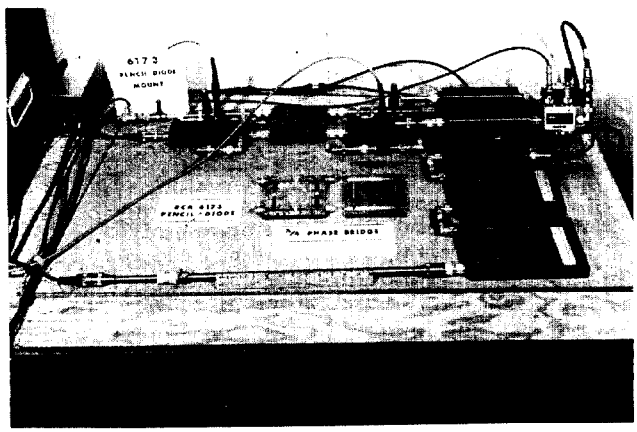

Fig. 3. Experimental 805-Mc phase detector, using $\lambda/4$ four-arm bridge with 6173 pencil diode detectors.

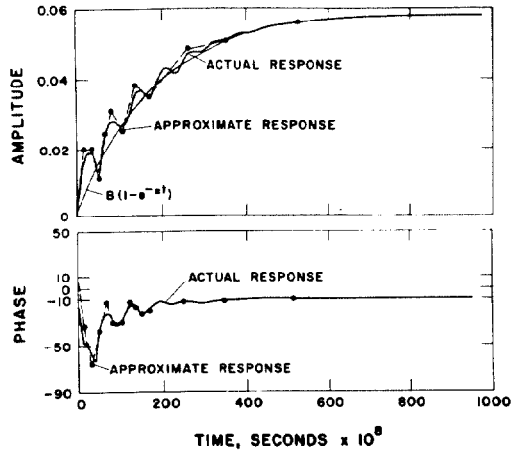

Fig. 4. Exact and approximate computed envelope responses of the RF field amplitude and phase in a typical cell to a pulse of pi-mode RF drive.

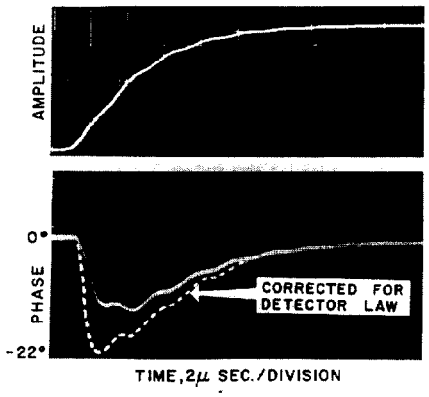

Fig. 5. Experimental responses of RF field amplitude and phase to a pulse of RF drive in an N = 20, Q = 11,800, k_{eff} = 0.10 cloverleaf structure driven at the pi-mode.

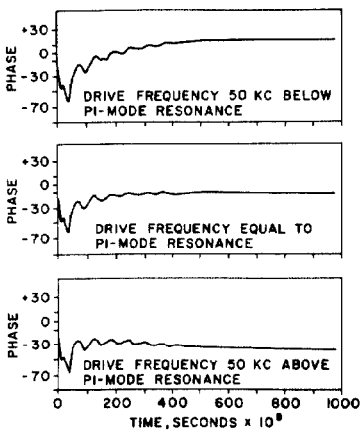

Fig. 6. Exact computed RF phase envelope responses to a pulse of RF drive.
a. Drive 50 kc below pi-mode resonance.
b. Drive at pi-mode resonance.
c. Drive 50 kc above pi-mode resonance.

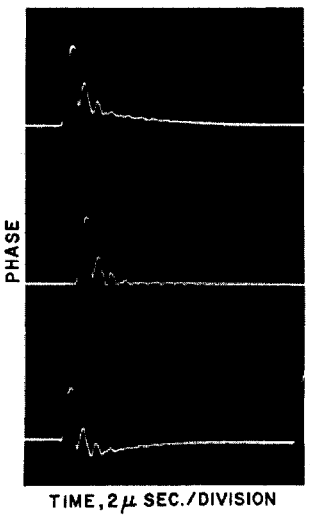

Fig. 7. Qualitative experimental RF phase responses in an N-22, Q = 10,700, k = 0.03, $\pi/2$-mode resonantly coupled side-cavity structure ("Mickey Mouse") to a pulse of RF drive. a. Drive 10 kc below $\pi/2$-mode resonance. b. Drive at $\pi/2$-mode resonance. c. Drive 10 kc above $\pi/2$-mode resonance.

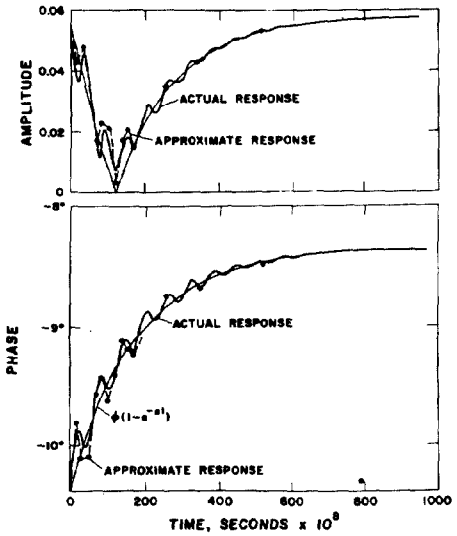

Fig. 8. Exact and approximate computed envelope responses of the RF phase and amplitude in a typical cell to a step change in the phase of the drive, occurring during the "flat" portion of the main pulse. a. Amplitude response to a 180° phase step. b. Phase response to a 2° phase step.

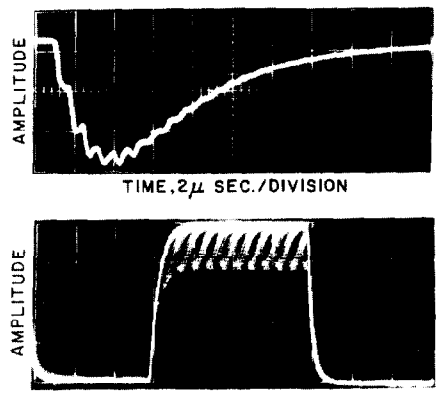

Fig. 9. Experimental response of RF field amplitude in the structure of Fig. 7 to a step phase change in the drive. a. Amplitude response to a 72° phase step. b. Amplitude disturbance due to 72° phase step shown on top of main drive pulse.

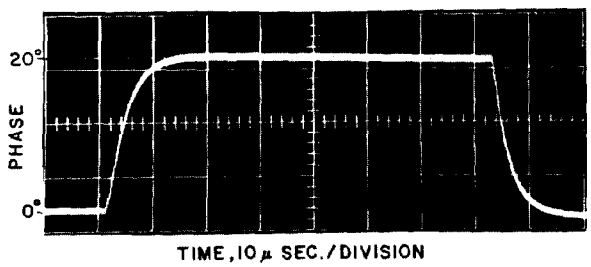

Fig. 10. Experimental response of RF phase in the structure of Fig. 7 to a 20° step change in the phase of the drive.